5/15/91 M.L.R. ①

UCRL-ID-106868

Evaluation Of Modified Log-Periodic Antennas For Pulse Transmission

Gerald J. Burke

April, 1991

Lawrence Livermore National Laboratory

Work performed under the auspices of the U.S. Department of Energy by the Lawrence Livermore National Laboratory under Contract W-7405-Eng-48.

EVALUATION OF MODIFIED LOG-PERIODIC ANTENNAS FOR PULSE TRANSMISSION

UCRL-ID--106868

DE91 011775

Introduction

The log-periodic dipole (LPD) antenna can operate over a very wide frequency band, limited only by mechanical constraints. However, the antenna is known to introduce significant distortion when radiating a transient signal, due to its nonlinear phase versus frequency response. A modified design has been proposed by Yatskevich and Fedosenko in [1] to reduce distortion of a pulse by making the phase response linear or, more generally, to develop a filter characteristic for compressing a signal such as a linear FM pulse. Some results from numerical modeling of these linear-phase and FM-compression antennas are presented here to evaluate their effectiveness.

Standard LPD antennas are constructed as an array of parallel dipoles arranged so that their ends subtend a constant angle α, as shown in Figure 1. The lengths of successive dipole elements form a geometric progression with scaling factor $\tau < 1$, so that

$$\frac{\ell_n}{\ell_{n-1}} = \frac{r_n}{r_{n-1}} = \frac{d_n}{d_{n-1}} = \tau. \tag{1}$$

The dipoles are fed with a transmission line that reverses phase between each pair of dipoles. Another parameter often used to describe a LPD antenna is

$$\sigma = \frac{d_n}{2\ell_n} = \left(\frac{1-\tau}{4}\right)\cot\alpha.$$

Thus σ is the distance in wavelengths from a $\lambda/2$ resonant element to the next smaller dipole in front of it.

A useful chart for initial design of LPD arrays was developed by Carrel [2], and is repeated in Figure 2. The line shown as optimum is the σ for which a given gain is achieved with a minimum τ. Carrel notes in [2] that for σ less than about 0.05 the directivity falls off rapidly, while too large a σ results in side lobes. For small values of τ, to the right of Figure 2, only one element is near $\lambda/2$ in length, so directivity is lost, and a substantial part of the energy passes the active region and is absorbed or reflected at the termination. Use of a large value for τ requires many elements to cover a specified band. The Livermore LPD antenna has $\tau = 0.788$ and $\sigma = 0.168$, so it is a low-gain design for maximum bandwidth with a minimum number of elements.

The Linear-Phase Antenna for Pulse Transmission

It is well known that when a transient signal is fed into a LPD antenna the radiated field is greatly distorted from the input pulse. Input of a short pulse, such as a Gaussian, results in a down-chirp radiated field. This effect is discussed in [3]. Yatskevich and Fedosenko note in [1] that this distortion is due to the nonlinear phase response of the standard LPD array. With the element ends subtending a constant angle, the distance in wavelengths of a resonant $\lambda/2$ element from the apex is constant. However, the radiated field changes phase by π radians when the frequency increases by a factor of τ due to the reversal of the transmission line between elements. Thus the phase of the radiated field varies as

$$\psi(\omega) = \frac{\pi}{\ln \tau} \ln(\omega/\omega_1).$$

Yatskevich and Fedosenko modified the antenna to produce a more linear phase characteristic. The resonant frequencies of successive elements in their antenna are related by an arithmetic progression with frequency increment $\delta\omega$, as

$$\omega_n = \omega_1 + (n-1)\delta\omega; \qquad n = 1, 2, \ldots, N$$

with element lengths

$$\ell_n = \ell_1/[1 + (n-1)\delta\omega/\omega_1]. \tag{2}$$

Since the elements in their antenna still subtend a constant angle α, the distance of the resonant element from the apex should remain constant over the band of the antenna. Thus the phase should change by π with a frequency increment of $\delta\omega$, so that

$$\psi(\omega) = -\pi\omega/\delta\omega.$$

This argument neglects the possible frequency-dependent phase velocity of the transmission line in the antenna, but results in [1] and here show that the antenna works reasonably well.

The effect of scaling the elements by Eq. (2) rather than Eq. (1) is to crowd the elements toward the small end with increased spacing for the large elements. The local values of both τ and σ, from the standard LPD definition, vary along the length of the modified antenna. Yatskevich and Fedosenko demonstrate their design for an antenna with 30 elements, $\delta\omega/\omega_1 = 0.1364$ and $\alpha = 10.5°$. The ratio of element radius to length was 0.01 and the transmission line impedance was 100 ohms. This antenna was modeled with the largest element scaled to match that of the Livermore LPD antenna. The position and size of the radiating elements are shown in Figure 3 and the dimensions are included in the Appendix. The smallest element was 0.85 times the length of the smallest element in the Livermore antenna, and the overall length was 1.78 times the length of the Livermore antenna.

This antenna was modeled in the frequency domain with the Moment-Method code NEC. In this model the radiating elements are broken into small segments, and the mutual interactions of all segments are computed to form an interaction matrix. The ideal transmission line equations are applied to establish a relation between voltage and current at the transmission line connection points. The combined system of transmission line and electromagnetic interaction equations is then solved to obtain the current throughout the antenna. Yatskevich and Fedosenko employ an equivalent method, described in [4]. From this solution we obtain the radiated field $E_0(\omega)$ of the antenna for unit voltage applied to the antenna terminals. The response with a source having impedance Z_s is then

$$E_s(\omega) = \frac{2Z_i(\omega)}{Z_i(\omega) + Z_s} E_0(\omega)$$

where $Z_i(\omega)$ is the input impedance of the antenna, and the generator produces one volt into a matched load. E_s represents a transfer function from which the impulse response can be obtained through an inverse Fourier transform.

The computed response of the 30 element antenna in Figure 3 is shown in Figure 4. The response in 4a, which represents E_0, was adjusted for a 50 ohm source impedance. The impulse response was then convolved with a Gaussian pulse with 1 ns FWHM to obtain the transient response in Figure 4d. It can be seen in Figure 4a that the phase is reasonably linear. The transient response in 4d is substantially more compressed in duration than the response that would be obtained from a normal LPD antenna. The dashed line on this and subsequent transient field plots represents the input Gaussian pulse with its amplitude in volts reduced by half so as not to change the plot scale for radiated field.

The effect of applying the linear scaling of Eq. (2) to an antenna like the Livermore LPD antenna is illustrated in Figure 5. Both antennas in the figure have seven elements with $\ell_1 = 0.88$ m and $\ell_7 = 0.21$ m with $\alpha = 17.5$ degrees. In the Livermore antenna the elements scale with $\tau = 0.788$. For the second antenna in Figure 5 the element lengths are determined by Eq. (2) with $\delta\omega/\omega_1 = 0.532$. The large spacing of the low frequency elements on this modified antenna would be expected to degrade the antenna performance. Hence another antenna design was considered for comparison. Keeping the largest and smallest elements the same as in the Livermore antenna, an optimum design was chosen from Figure 2 for a gain of 10 dB. The result was $\tau = 0.915$, $\sigma = 0.168$ and $\alpha = 7.21$ degrees. With this τ, 18 elements are needed to cover the band of the Livermore antenna. A comparable linear-phase antenna used 18 elements with the same largest and smallest elements, and the same α, but with element lengths determined from Eq. (2) with $\delta\omega/\omega_1 = 0.207$. These two 18 element antennas are shown in Figure 6.

The responses of the seven element antennas in Figure 5 are compared in Figures 7 and 8. The transfer function of the linear-phase antenna in Figure 8 may be somewhat more linear than that of the standard LP, but the magnitude at low frequencies is reduced by the large element spacing. The transient response of the linear-phase antenna is more compressed than that of the LP, but there is only a small increase in the peak field strength.

Comparison of the 18 element LPD and linear-phase antennas in Figures 9 and 10 shows a considerably more linear phase response for the modified antenna. The transient response in Figure 10 is compressed, and its peak amplitude exceeds that of the standard LPD antenna in Figure 9 by a factor of nearly two. The response of the 30 element linear-phase antenna in Figure 4 is similar to that in Figure 10, but with a somewhat higher peak field.

Pulse Compression Antennas

Yatskevich and Fedosenko show that this concept of tailoring the phase response of the antenna can be generalized by selecting the resonant frequencies ω_n of the radiating elements to obtain a phase response

$$\psi(\omega_n) = \psi(\omega_1) - (n-1)\pi. \tag{3}$$

They apply this method to compress a linear FM signal of the form

$$u(t) = \begin{cases} u_0 \cos\left(\omega_0 t + \frac{\Delta\omega^2 t^2}{2B}\right), & \text{for } |t| \le t_u/2, \\ 0, & \text{for } |t| > t_u/2, \end{cases}$$

where ω_0 is the mean frequency, t_u is the duration of the signal, $\Delta\omega$ is the bandwidth and $B = \Delta\omega t_u$. The spectrum of this signal, assuming $B \gg 1$, is

$$U(\omega) \approx u_0 \frac{\sqrt{\pi B/2}}{\Delta\omega} e^{-j\frac{B(\omega-\omega_0)^2}{2\Delta\omega^2}} \tag{4}$$

over the frequency range $\omega_0 - \Delta\omega/2 < \omega < \omega_0 + \Delta\omega/2$.

The antenna is required to act as an optimum filter, with the conjugate phase response to Eq. (4). Thus

$$\psi(\omega) = B(\omega - \omega_0)^2/2\Delta\omega^2 - \omega t_0 \tag{5}$$

where t_0 is a time delay chosen to obtain a realizable antenna. Substituting Eq. (5) into Eq. (3) and solving for ω_n yields

$$\omega_n = \omega_0 + \frac{\Delta\omega t_0}{t_u}\left\{1 - \sqrt{1 - \frac{2t_u}{\Delta\omega t_0^2}\left[t_0(\omega_1 - \omega_0) - \frac{t_u}{2\Delta\omega}(\omega_1 - \omega_0)^2 + (n-1)\pi\right]}\right\}$$

Assuming $\omega_0 = \omega_1 + \Delta\omega/2$ as in [1], this result becomes

$$\omega_n = \omega_1\left[1 + \frac{\Delta\omega}{\omega_1}\left(0.5 + \gamma - \sqrt{(0.5+\gamma)^2 - 2\pi(n-1)/B}\right)\right]$$

where $\gamma = t_0/t_u$. Thus the element lengths scale as

$$\ell_n = \ell_1\Big/\left[1 + \frac{\Delta\omega}{\omega_1}\left(0.5 + \gamma - \sqrt{(0.5+\gamma)^2 - 2\pi(n-1)/B}\right)\right] \tag{6}$$

Yatskevich and Fedosenko consider a linear FM signal with $B = 40\pi$ and $\Delta\omega/\omega_0 = 1$. Their antenna uses 30 elements with $\alpha = 4°$ and $\gamma = 0.705$. The ratio of element radius to length was 0.005, and the transmission line impedance was 100 ohms. The antenna modeled here was scaled so that the longest element was equal to that of the Livermore antenna. Thus $f_1 = 0.170$ GHz and $f_{30} = 0.511$ GHz. The radiating elements of this antenna are shown in Figure 11 and the element dimensions are included in the Appendix.

The response of the antenna, obtained from NEC, is shown in Figure 12, and the input linear FM signal and the field radiated are shown in Figure 13. The radiated pulse is compressed, but not as well as that shown by Yatskevich and Fedosenko in [1]. One uncertainty in this comparison is the source impedance, since a value is not stated in [1]. In addition to the 50 ohms used for the results in Figure 13, we also tried 100 and 1000 ohms. The high impedance was tried because reference [4] mentions fixing the input current, which is equivalent to using a high impedance source. These variations in source impedance did not have a significant effect on the compression of the radiated pulse, although they did alter its amplitude.

The result of convolving the linear FM signal with the impulse response of the optimum filter, having the phase of Eq. (5) and a constant amplitude from $\omega_0 - \Delta\omega/2$ to $\omega_0 + \Delta\omega/2$, is shown in Figure 14. This response is close to that shown in [1]. The transfer function of the antenna, computed by NEC, is compared with the ideal transfer function in Figure 15. The magnitude of the antenna response is seen to drop off sharply above about 0.34 GHz. This loss of high frequencies is also noted by Yatskevich and Fedosenko, and the gain in Figure 12b appears to be in close agreement with that shown in [1]. The phase of the antenna response is not plotted in [1], but it is stated that the phase is within ± 10 degrees of the quadratic relation of Eq. (5). The phase computed by NEC is close to that of Eq. (5) at the lower frequencies, but deviates substantially above about 0.32 GHz. This difference in phase apparently accounts for the reduced compression of the pulse. The phase characteristic is more difficult to obtain than the smoothly varying magnitude, since many samples are needed to avoid aliasing. The computation of the transfer function shown in Figure 12, from 0 to 1 GHz, required 12 hours of CPU time on a VAX 8650.

For further comparison, the response of the 18 element log-periodic and linear-phase antennas in Figure 6 with input of the linear FM pulse are shown in Figure 16. The uniform log-periodic antenna shows some pulse compression at low frequencies, as might be expected from the down-chirp characteristic of its impulse response. However, the compression is not as great as in Figure 13.

Conclusions

The concept of modifying a LPD array to produce a desired phase characteristic for transmitting or compressing a pulse appears to have considerable merit, although there are limitations on what can be achieved. The linear-phase modification proposed in [1] is effective for radiating a short pulse with minimum dispersion. However, more elements are needed to cover a given band than with the standard LPD array.

The antenna for compression of a linear FM pulse also is effective, although the radiated pulse obtained from the NEC model is not as clean as that shown in [1]. The reason for this discrepancy has not been determined, although it appears possible that the pulse shown in [1] could be the response of the ideal filter, which is then broadened by the reduced bandwidth of the antenna. Statements in [1] appear somewhat ambiguous on this point. Another possibility is that the result shown in [1] is for a different antenna than is described.

The simple analysis used in deriving the element spacings in [1] probably does not lead to a completely optimum design. The antennas might be further optimized by adjusting the elements to correct phase errors revealed by the numerical model, although the potential gain is not known. Also, an analysis in terms of $k - \beta$ diagrams for propagation on the locally-periodic structure might lead to a better understanding of the possibilities and limitations of these antennas.

References

[1] V. A. Yatskevich and L. L. Fedosenko, "Antennas for Radiation of Very-Wide-Band Signals," *Radio Electronics and Communication Systems*, Vol. 29, No. 2, pp. 62-66, 1986.

[2] R. Carrel, "The Design of Log-Periodic Dipole Antennas," *IRE International Convention Record*, Vol. I, pp. 61-75, 1961.

[3] C. M. Knop, "On Transient Radiation from a Log-Periodic Dipole Array," *IEEE Trans. on Antennas and Propag.*, AP-18, No. 6, pp. 807-809, November 1970.

[4] V. A. Yatskevich and V. M. Lapitskij, "Exact and Approximate Methods of Calculating Log-Periodic Dipole Antennas," *Radio Electronics and Communication Systems*, Vol. 22, No. 5, pp. 64-67, 1979.

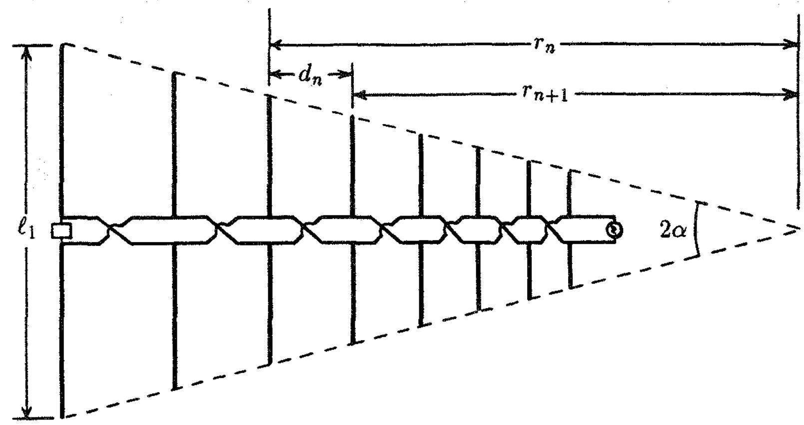

Fig. 1. Log-periodic dipole antenna geometry.

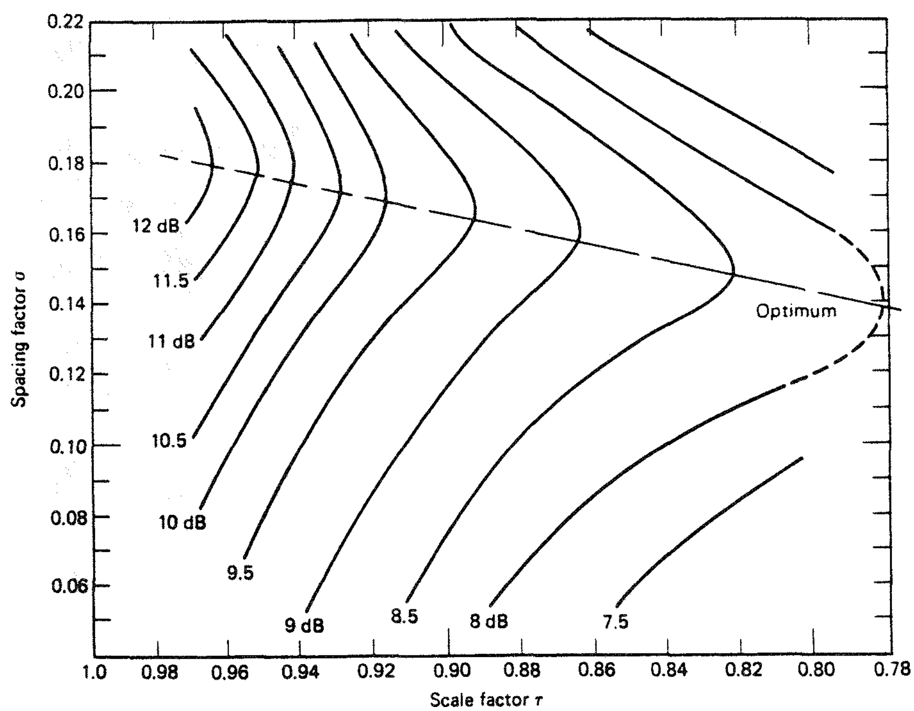

Fig. 2. Gain of a LPD array versus τ and σ, from Carrel [2]. The transmission line impedance is Z_c = 100 ohms, and ℓ_n/a_n = 250 where a_n is the radius of element n.

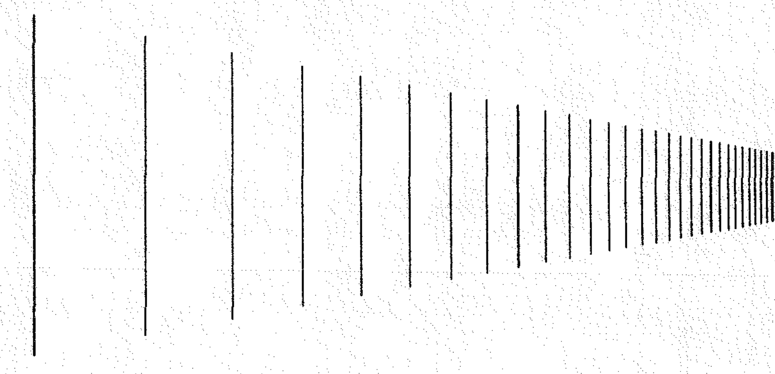

Fig. 3. Radiating elements of a linear-phase antenna with $N = 30$, $\delta\omega/\omega_1 = 0.1364$ and $\alpha = 10.5°$.

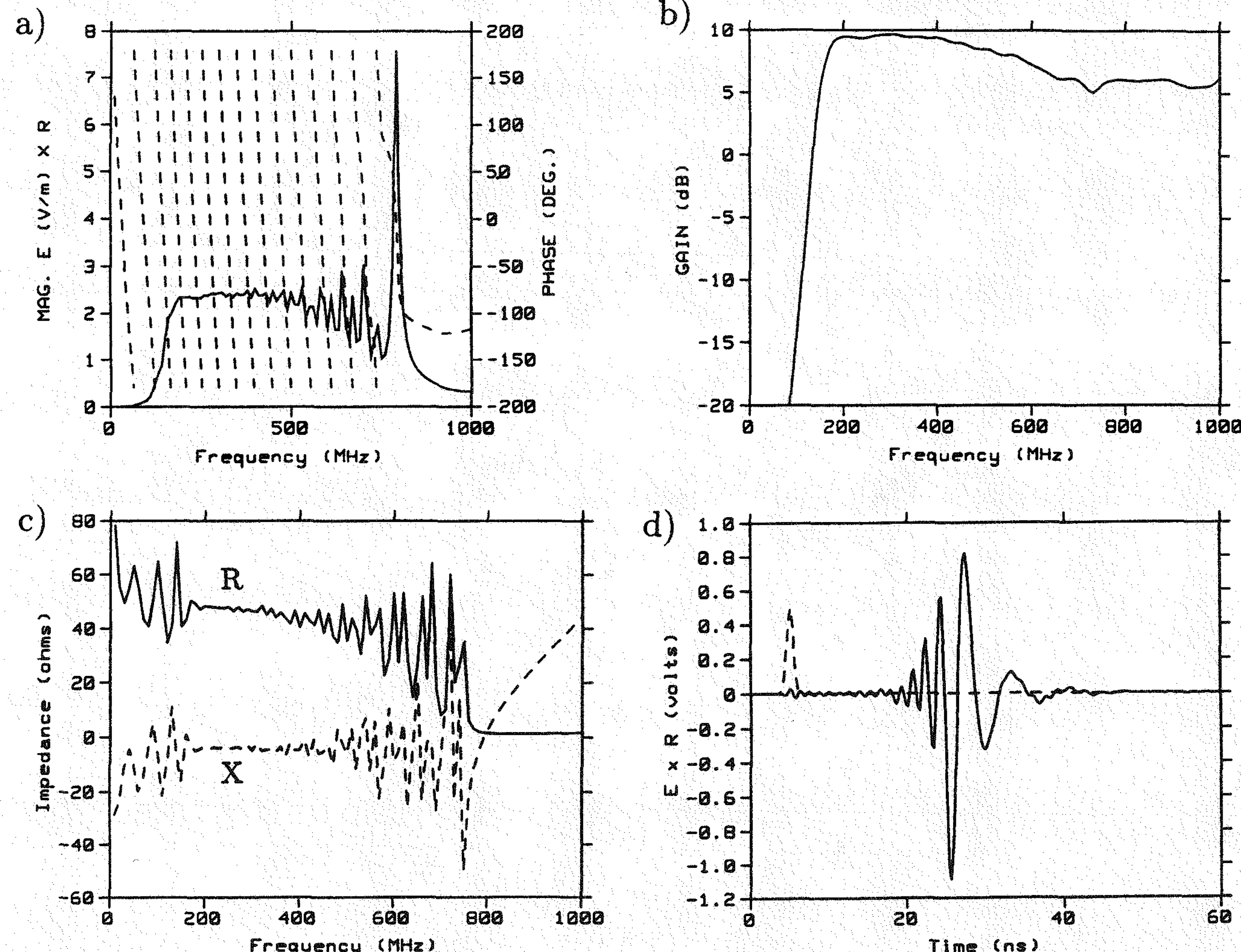

Fig. 4. Response of the 30 element linear-phase antenna from Figure 3, showing a) radiated field magnitude (———) and phase (- - - -) on axis for one volt input, b) power gain relative to an isotropic source, c) input impedance and d) transient radiated field on axis for an input Gaussian pulse with one volt amplitude and 1.0 ns FWHM.

a)

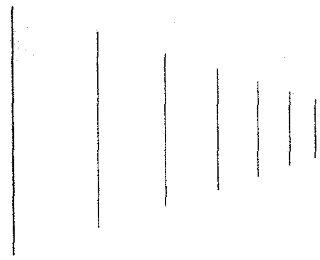

b)

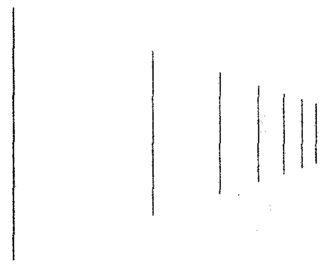

Fig. 5. Radiating elements of a) the Livermore LPD antenna with $\tau = 0.788$, $\sigma = 0.168$ and $\alpha = 17.5°$ and b) a similar linear-phase antenna with $\delta\omega/\omega_1 = 0.532$.

a)

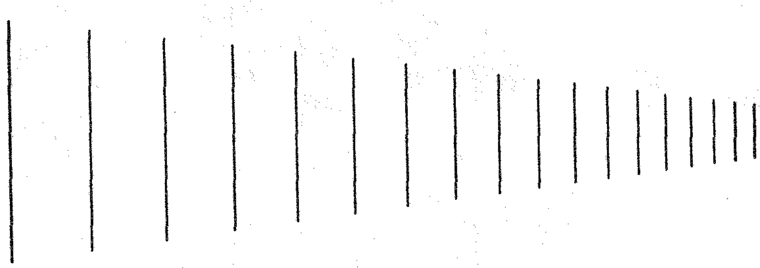

b)

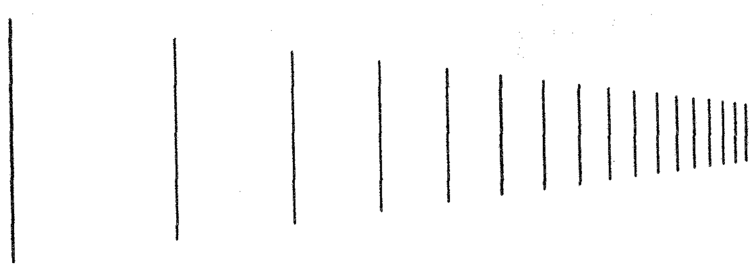

Fig. 6. Radiating elements of a) an 18 element LPD antenna covering the band of the Livermore antenna, with $\tau = 0.915$, $\sigma = 0.168$ and $\alpha = 7.21°$ and b) a similar linear-phase antenna with $\delta\omega/\omega_1 = 0.207$.

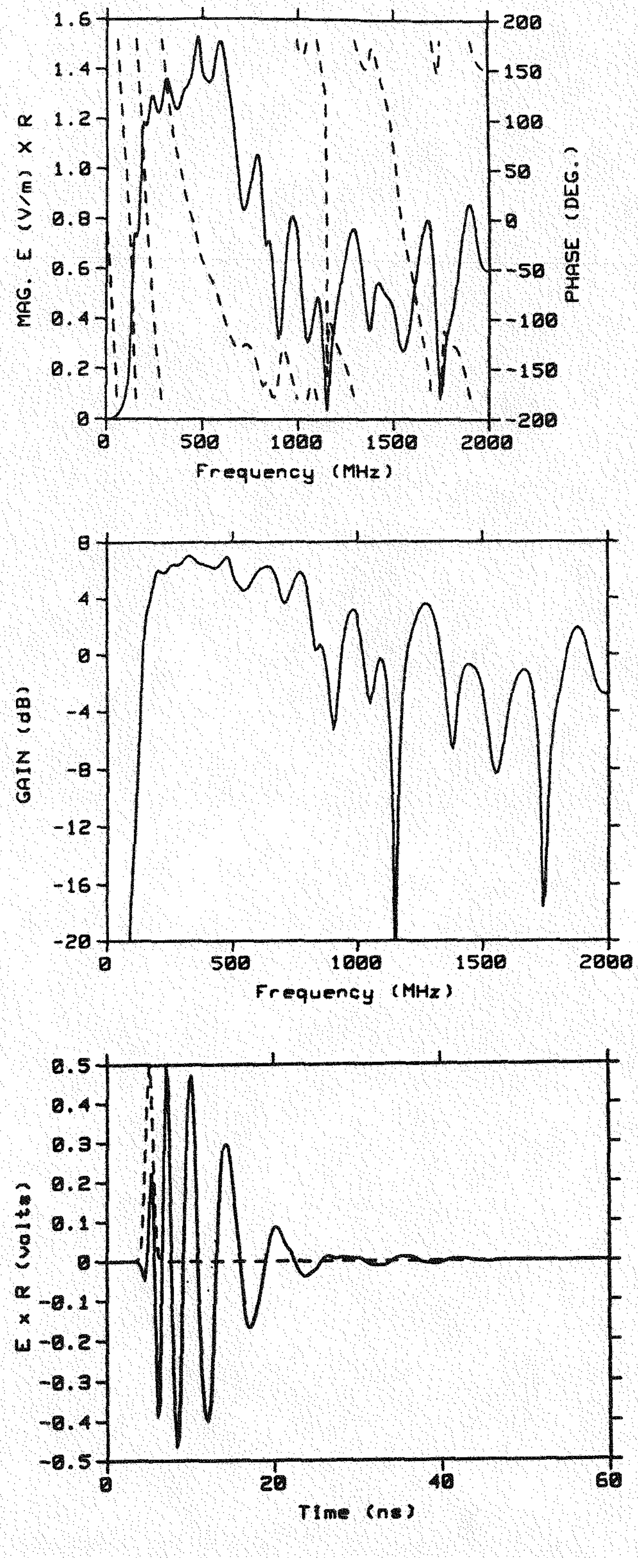

Fig. 7. Response of a 7 element log-periodic antenna from Fig. 5, with $\tau = 0.788$. Shown are radiated field magnitude (———) and phase (- – – –), power gain and transient response to a Gaussian pulse with 1 ns FWHM.

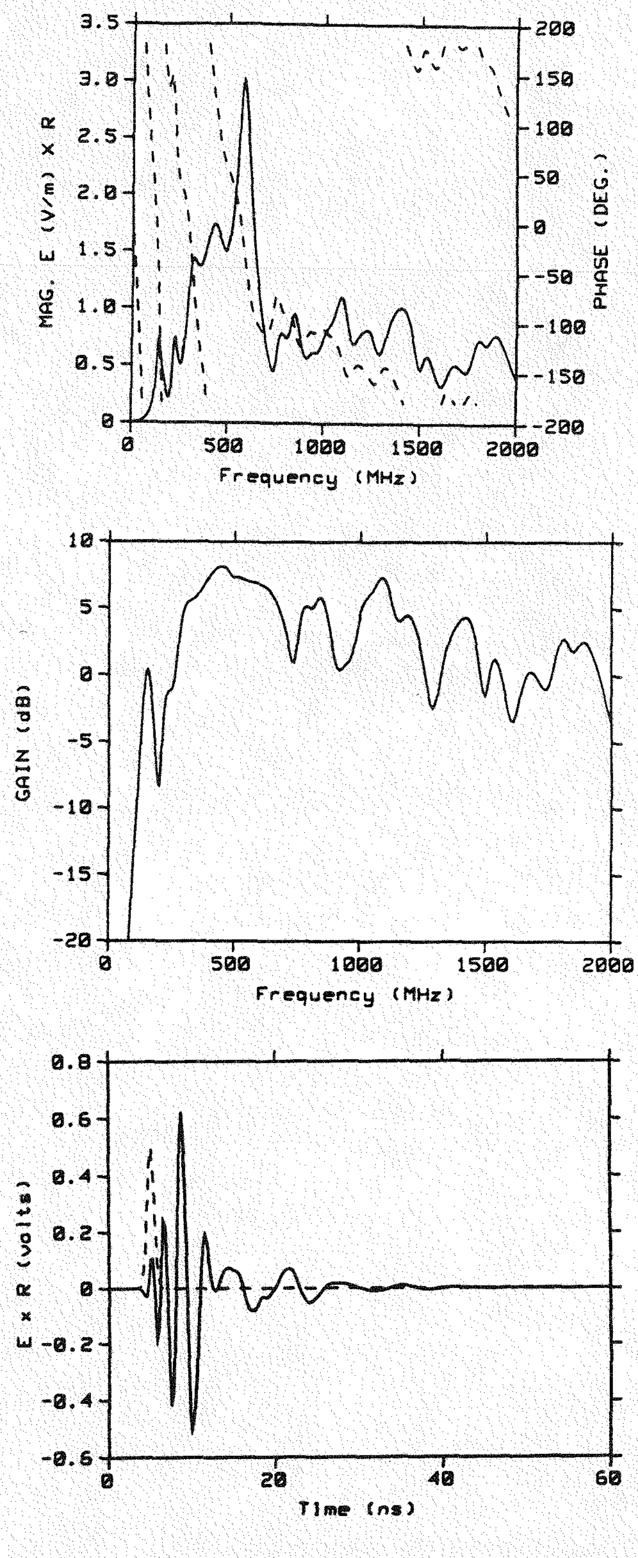

Fig. 8. Response of a 7 element linear-phase antenna from Fig. 5. Shown are radiated field magnitude (———) and phase (– – –), power gain and transient response to a Gaussian pulse 1 ns FWHM.

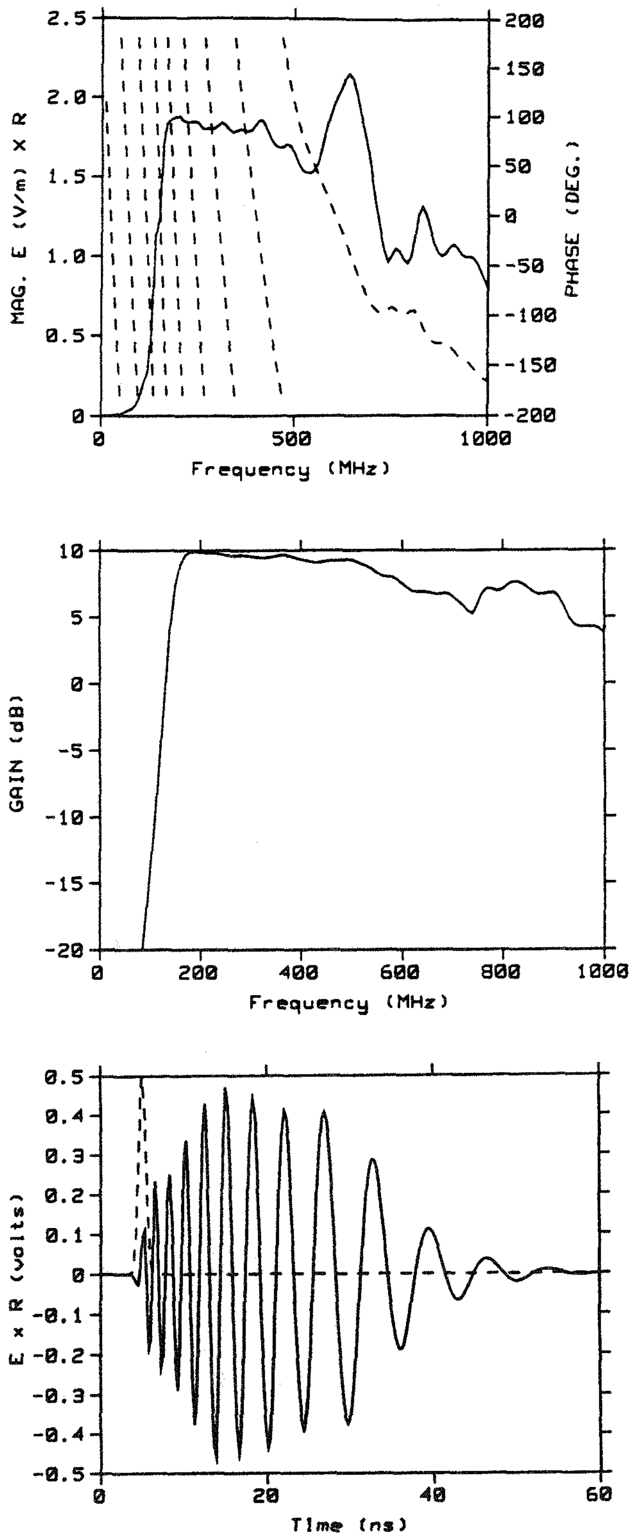

Fig. 9. Response of an 18 element log periodic antenna from Fig. 6, with $\tau = 0.915$. Shown are radiated field magnitude (———) and phase (– – –), power gain and transient response to a Gaussian pulse 1 ns FWHM.

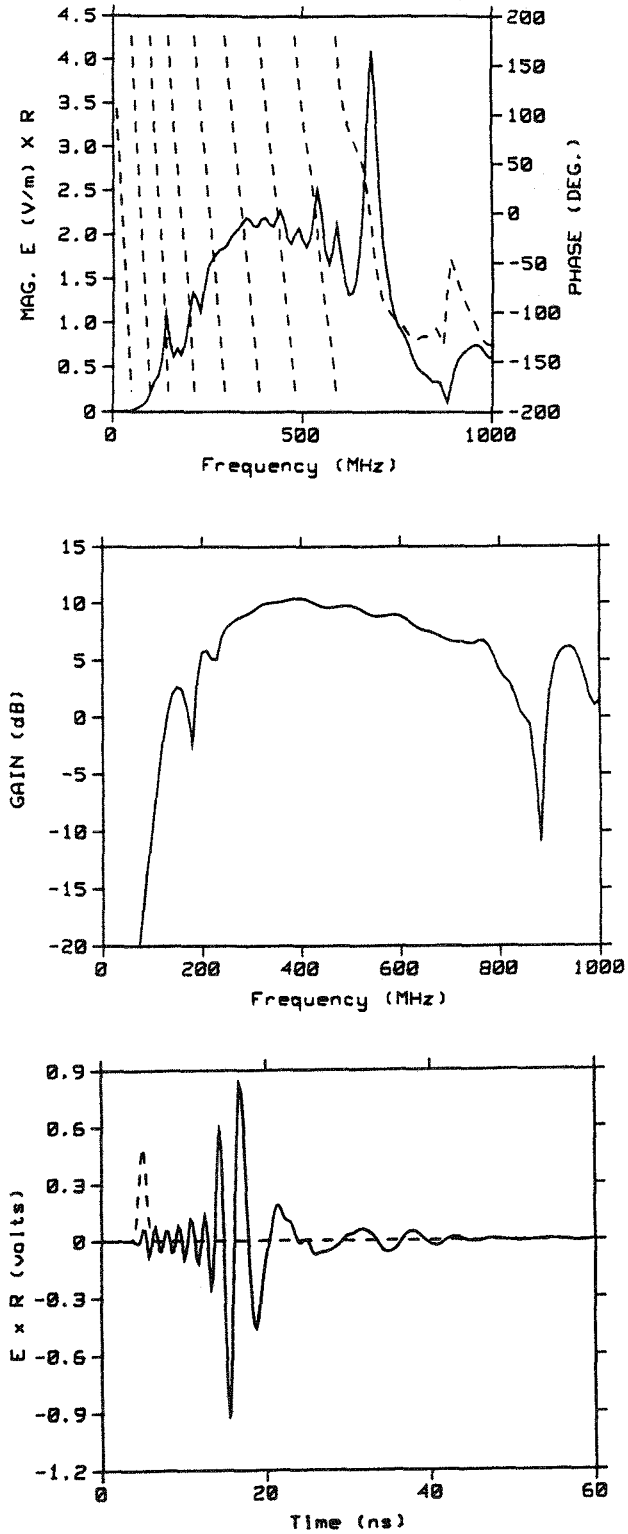

Fig. 10. Response of an 18 element linear phase antenna from Fig. 6. Shown are radiated field magnitude (———) and phase (- - - -), power gain and transient response to a Gaussian pulse 1 ns FWHM.

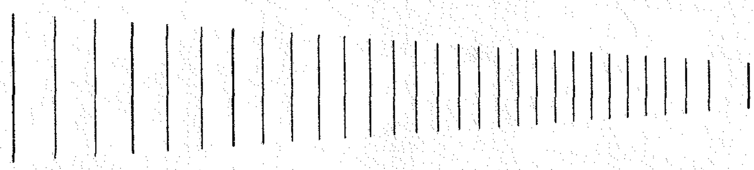

Fig. 11. Radiating elements of a thirty-element antenna for compressing a linear FM pulse, with $\Delta\omega/\omega_1 = 2$, $B = 40\pi$ and $\gamma = 0.705$.

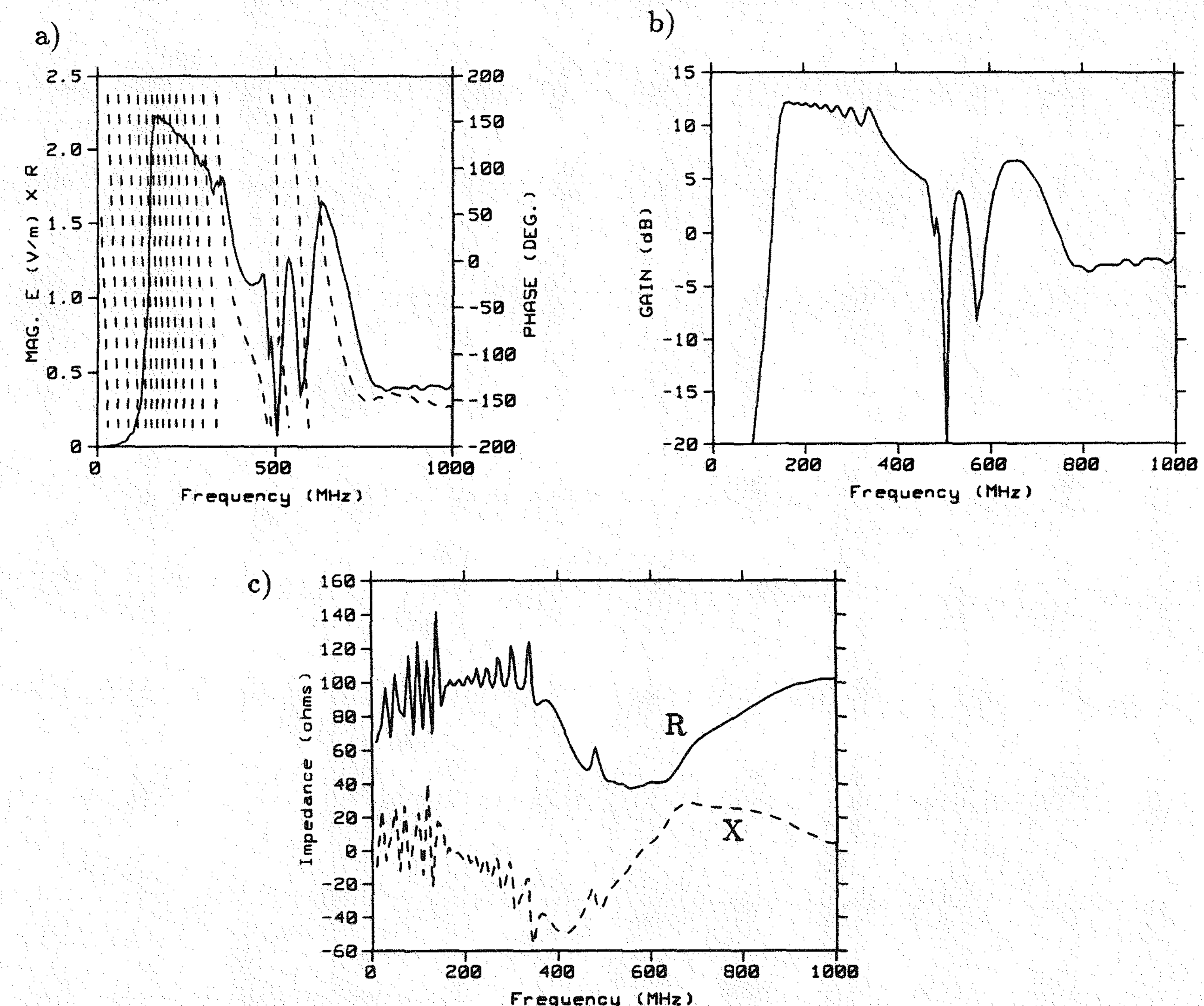

Fig. 12. Frequency response of the thirty-element antenna in Figure 11, showing a) radiated field magnitude (———) and phase (- - - -) on axis for one volt input, b) power gain relative to an isotropic source and c) input impedance.

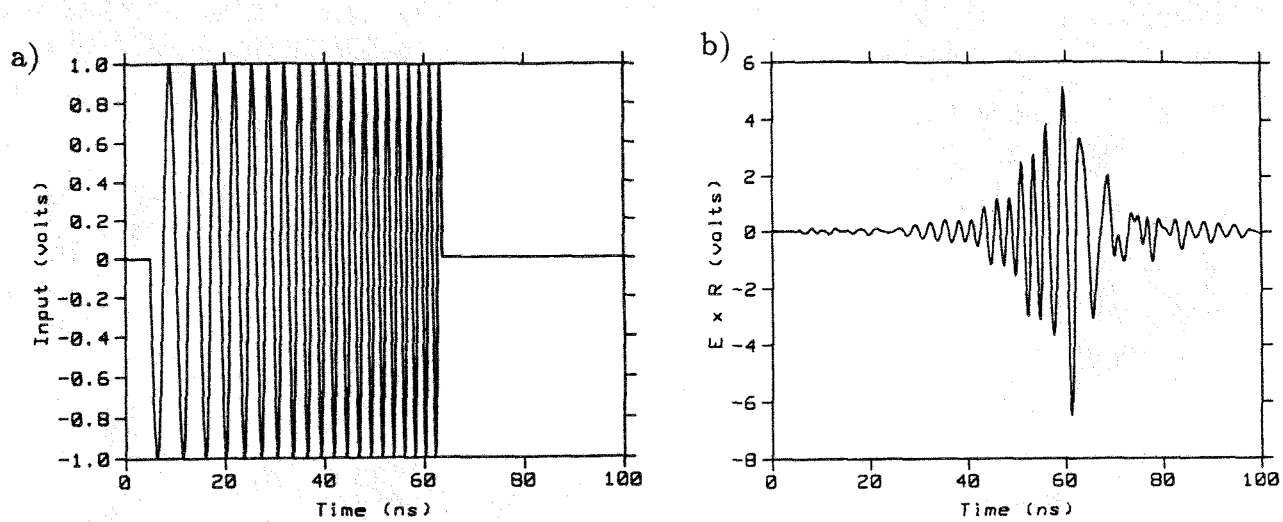

Fig. 13. Transient response of the pulse compression antenna of Figure 11, showing a) linear FM input pulse with $f_0 = \Delta f = 0.34091$ GHz and $t_u = 58.667$ ns and b) radiated field of the antenna on axis.

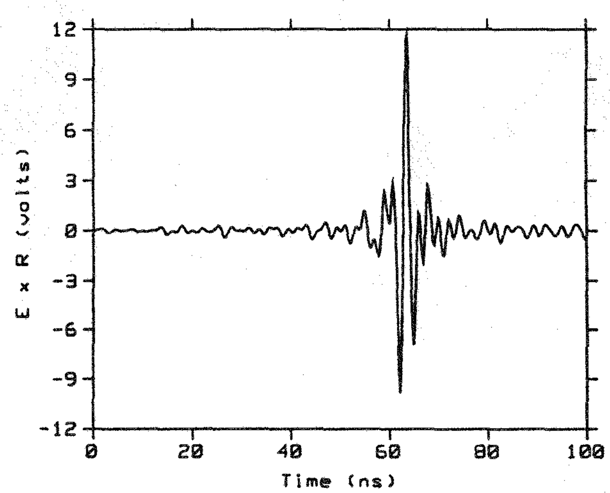

Fig. 14. Result of convolving a linear FM signal with $f_0 = \Delta f = 0.34091$ GHz and $t_u = 58.667$ ns with the optimum filter response having the phase of Eq. (5).

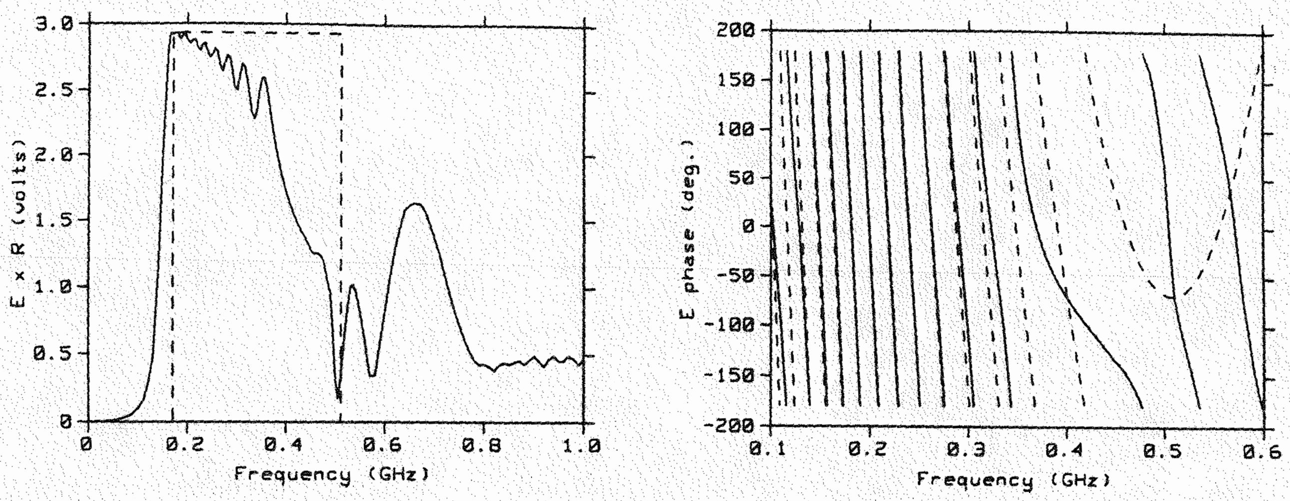

Fig. 15. Comparison of the response of the pulse compression antenna in Figure 11 computed by NEC for a 50 ohm source (———) with the optimum-filter response (– – – –).

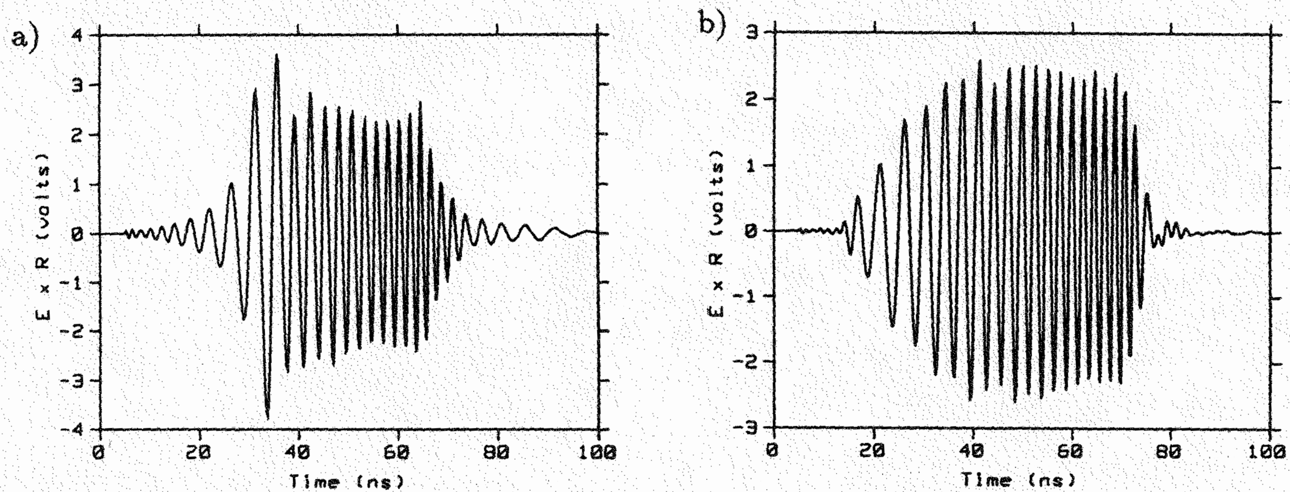

Fig. 16. Radiated field of a) the 18-element log-periodic antenna and b) the linear-phase antenna from Figure 6 for input of the linear FM pulse from Figure 13a.

APPENDIX
Antenna Dimensions

Dimensions of the log-periodic and modified log-periodic antennas are given below. All lengths are in meters. For antennas that are not log periodic the local parameters comparable to a log-periodic antenna are given as $\tau_n = \ell_{n+1}/\ell_n$ and $\sigma_n = 0.25(1 - \tau_n)\cot\alpha$.

Table 1. Seven element linear-phase antenna, with $\alpha = 17.5°$ and $\delta\omega/\omega_1 = 0.5317$. The radius of element n was $\ell_n/100$ and the transmission line impedance was 100 ohms.

n	$\ell_n/2$	$r_n - r_7$	τ_n	σ_n
1	0.4400	1.0625	0.6529	0.2752
2	0.2873	0.5782	0.7423	0.2043
3	0.2132	0.3432	0.7951	0.1625
4	0.1695	0.2046	0.8300	0.1348
5	0.1407	0.1132	0.8547	0.1152
6	0.1203	0.0485	0.8731	0.1006
7	0.1050	0.0000		

Table 2. Eighteen element log-periodic antenna, with $\tau = 0.915$, $\sigma = 0.168$ and $\alpha = 7.21°$. The radius of element n was $\ell_n/100$ and the transmission line impedance was 100 ohms.

n	$\ell_n/2$	$r_n - r_{18}$
1	0.4400	2.7101
2	0.4026	2.4144
3	0.3684	2.1439
4	0.3371	1.8963
5	0.3084	1.6698
6	0.2822	1.4626
7	0.2582	1.2729
8	0.2363	1.0994
9	0.2162	0.9407
10	0.1978	0.7954
11	0.1810	0.6625
12	0.1656	0.5408
13	0.1515	0.4295
14	0.1387	0.3277
15	0.1269	0.2345
16	0.1161	0.1493
17	0.1062	0.0713
18	0.0972	0.0000

Table 3. Eighteen element linear-phase antenna, with $\alpha = 7.21°$ and $\delta\omega/\omega_1 = 0.20746$. The radius of element n was $\ell_n/100$ and the transmission line impedance was 100 ohms.

n	$\ell_n/2$	$r_n - r_{18}$	τ_n	σ_n
1	0.4400	2.7101	0.8282	0.3396
2	0.3644	2.1124	0.8534	0.2898
3	0.3110	1.6903	0.8721	0.2527
4	0.2712	1.3756	0.8866	0.2241
5	0.2405	1.1329	0.8982	0.2013
6	0.2160	0.9392	0.9076	0.1827
7	0.1960	0.7811	0.9154	0.1672
8	0.1794	0.6499	0.9220	0.1542
9	0.1654	0.5392	0.9276	0.1430
10	0.1535	0.4451	0.9325	0.1334
11	0.1431	0.3629	0.9368	0.1249
12	0.1341	0.2917	0.9405	0.1175
13	0.1261	0.2285	0.9439	0.1109
14	0.1190	0.1723	0.9469	0.1050
15	0.1127	0.1225	0.9495	0.0997
16	0.1070	0.0775	0.9520	0.0949
17	0.1019	0.0372	0.9542	0.0906
18	0.0972	0.0000		

Table 4. Thirty element linear-phase antenna, with $\alpha = 10.5°$ and $\delta\omega/\omega_1 = 0.1364$. The radius of element n was $\ell_n/100$ and the transmission line impedance was 100 ohms.

n	$\ell_n/2$	$r_n - r_{30}$	τ_n	σ_n
1	0.4400	1.8950	0.8800	0.1619
2	0.3872	1.6100	0.8928	0.1446
3	0.3457	1.3861	0.9032	0.1306
4	0.3122	1.2056	0.9117	0.1190
5	0.2847	1.0569	0.9189	0.1094
6	0.2616	0.9324	0.9250	0.1012
7	0.2420	0.8265	0.9302	0.0941
8	0.2251	0.7354	0.9348	0.0880
9	0.2104	0.6562	0.9388	0.0826
10	0.1975	0.5867	0.9423	0.0778
11	0.1861	0.5252	0.9454	0.0736
12	0.1760	0.4704	0.9483	0.0698
13	0.1669	0.4213	0.9508	0.0663
14	0.1587	0.3770	0.9531	0.0632
15	0.1512	0.3369	0.9552	0.0604
16	0.1445	0.3003	0.9571	0.0578
17	0.1383	0.2669	0.9589	0.0554
18	0.1326	0.2363	0.9605	0.0523
19	0.1273	0.2080	0.9620	0.0512
20	0.1225	0.1819	0.9634	0.0494
21	0.1180	0.1578	0.9647	0.0476
22	0.1139	0.1353	0.9659	0.0460
23	0.1100	0.1143	0.9670	0.0445
24	0.1064	0.0948	0.9681	0.0431
25	0.1030	0.0765	0.9691	0.0417
26	0.0998	0.0593	0.9700	0.0405
27	0.0968	0.0431	0.9709	0.0393
28	0.0940	0.0279	0.9717	0.0382
29	0.0913	0.0136	0.9725	0.0371
30	0.0888	0.0000		

Table 5. Thirty element antenna for compressing a linear FM pulse, with $\alpha = 4°$, $B = 40\pi$, $\gamma = t_0/t_u = 0.705$, $f_1 = 0.1745$ GHz and $f_0 = \Delta f = 0.34091$ GHz. The radius of element n was $\ell_n/200$ and the transmission line impedance was 100 ohms.

n	$\ell_n/2$	$r_n - r_{30}$	τ_n	σ_n
1	0.4400	4.3970	0.9598	0.1436
2	0.4223	4.1442	0.9607	0.1405
3	0.4057	3.9069	0.9615	0.1376
4	0.3901	3.6836	0.9622	0.1350
5	0.3754	3.4730	0.9629	0.1326
6	0.3615	3.2739	0.9635	0.1304
7	0.3483	3.0854	0.9641	0.1285
8	0.3358	2.9063	0.9645	0.1268
9	0.3239	2.7361	0.9650	0.1253
10	0.3125	2.5738	0.9653	0.1240
11	0.3017	2.4188	0.9656	0.1229
12	0.2913	2.2704	0.9659	0.1221
13	0.2813	2.1282	0.9660	0.1214
14	0.2718	1.9915	0.9661	0.1210
15	0.2626	1.8600	0.9662	0.1209
16	0.2537	1.7330	0.9661	0.1210
17	0.2451	1.6101	0.9660	0.1215
18	0.2368	1.4910	0.9658	0.1223
19	0.2287	1.3751	0.9654	0.1236
20	0.2208	1.2620	0.9649	0.1254
21	0.2130	1.1513	0.9643	0.1278
22	0.2054	1.0425	0.9634	0.1310
23	0.1979	0.9348	0.9621	0.1354
24	0.1904	0.8276	0.9605	0.1413
25	0.1829	0.7200	0.9581	0.1496
26	0.1752	0.6106	0.9547	0.1619
27	0.1673	0.4971	0.9491	0.1819
28	0.1588	0.3754	0.9382	0.2211
29	0.1490	0.2350	0.8897	0.3943
30	0.1325	0.0000		